A cavity model of the indentation hardness of a coated substrate

I. J. Ford

Theoretical Studies Department, AEA Industrial Technology, B424 4, Harwell Laboratory, Didcot, Oxon. OX11 0RA (UK)

(Received October 22, 1993; accepted December 8, 1993

Abstract

A simple model is proposed which predicts the hardness of a coated substrate as a function of coating thickness and indentation depth. The model is based on an analytical solution for the stress and strain fields around a pressurized coated spherical cavity, taking into account elastic and perfectly plastic deformation. The predictions of the coated cavity model can be applied to the plane coated surface by making various geometrical correspondences, and the model shows good agreement with finite-element calculations and experimental results for the case of a hard film on a soft substrate. For the less important case of a soft film on a harder substrate the cavity model is less successful for the plane coated surface geometry, owing to bulging at the free surface.

1. Introduction

One of the most important emerging areas in tribology is the use of coatings to alter the properties of surfaces (see for example refs. 1–3). A suitable choice of coating material can improve the mechanical or chemical nature of the surface, whilst retaining the desirable bulk properties of the substrate. For example, it might be advantageous to fashion a cutting tool out of a cheap, easily formed material and then to harden its surface by coating it thinly with a more expensive material. Alternatively, a coating might be used to improve the corrosion resistance of the surface of a component.

Theory can make an important contribution toward optimizing the properties of the coated substrate. The aim of this paper is to account for the dependence of the effective hardness on the depth of indentation into the surface. For very large indentations, the hardness of the coated surface should be approximately equal to the hardness of the substrate material. Conversely, for small indentation depths, the surface should respond with the hardness of the film material. For intermediate depths, the hardness will lie somewhere between the two limits. Theory can determine this behaviour and characterize how and under what conditions the coating can affect the surface properties. An appropriate coating thickness might then be selected according to the requirements of the application.

The problem has already been approached in a number of ways. Perhaps the definitive treatment is to model the elastoplastic deformation of the coated substrate numerically using finite elements [4] together with appropriate constitutive laws. This approach has a number of advantages, but calculations are cumbersome and expensive, and the results are specific to the properties of the materials modelled. It is arguably more useful to have available an approximate treatment, based on simple analysis, which can be used quickly to give hardness estimates, and which can be used to generalize behaviour, and to identify trends.

A number of such models have been proposed and used for this purpose [5–12]. However, some of the models are semiempirical and lack a rigorous analytical basis, while others are applicable only for linear materials [13, 14]. Furthermore, fitting parameters are sometimes necessary. In this paper a new model is proposed, based on the elastoplastic stress–strain solution for a pressurized coated spherical cavity. Similar approaches, based on an uncoated cavity, have been used to account for the hardness trends of uncoated substrates [15–20], and so it is a natural step to extend the method to include a coating. The results of the analysis are then applied to the real situation by a suitable mapping of the geometry.

In the following section, some previous models are reviewed briefly. In Section 3 the analysis of the pressurized coated spherical cavity is given, and the model is then applied to the indentation of plane coated substrates in Section 4, which includes comparisons with finite element calculations, other analytical models and real data. The model is discussed in Section 5 and conclusions are given in Section 6.

2. Models of coated surface hardness

Two models have previously been developed to provide simple estimates of the composite hardness of a coated substrate. The first of these, due to Jönsson and

SSDI 0040-6090(93)06004-Q

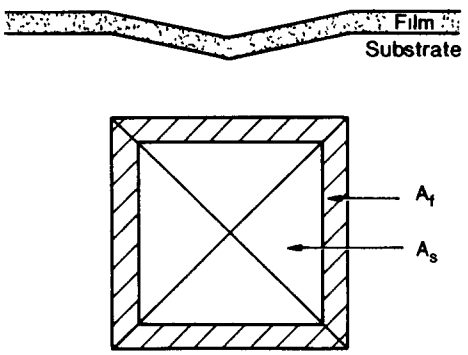

Fig 1 Geometry of indentation (for pyramidal indenter) used in area mixture law of composite hardness proposed by Jonsson and Hogmark [6] The film supports part of the load only at the margin of the indentation, within area A_f

Hogmark [6], uses a geometrical approach to combine the hardness of film and substrate according to an area mixture model. The approach is illustrated in Fig. 1. The film is considered to provide support only at the margin of the indentation area; elsewhere, it is assumed that the film is cracked and transmits the load directly onto the substrate. The composite hardness is given by

$$H_c = \frac{A_f}{A} H_f + \frac{A_s}{A} H_s \tag{1}$$

where A_f and A_s are the supporting areas, $A = A_f + A_s$, and H_f and H_s are the hardness of the film and substrate materials respectively. An analysis of the geometry [6] leads to

$$H_c = H_s + \left[\frac{2Ch}{d} - C^2\left(\frac{h}{d}\right)^2\right](H_f - H_s) \tag{2}$$

where h is the thickness of the coating, d is the depth of indentation and C is equal to $2\sin^2 11° = 0.073$ if $H_f \gg H_s$, or $\sin^2 22° = 0.14$ if $H_f \approx H_s$, for a Vickers pyramidal indenter with an angle of 136° between opposing faces. However, the model is unsuitable for indentation depths less than the film thickness, since it relies on film cracking to transmit load directly onto the substrate over the central part of the contact area.

In the second model, known as the volume mixture model [7–11], the hardness of film and substrate are combined according to the volumes of plastically deformed materials:

$$H_c = \frac{V_f}{V} H_f + \frac{V_s}{V} H_s \tag{3}$$

In an early version of the model [8], plasticity was assumed to be confined to a hemisphere of radius equal to the radius of the indentation impression at the surface (for a conical indenter), of volume V, containing the film and the substrate plastic volumes V_f and V_s. It was assumed that the indenter penetrated the film as shown in Fig. 2(a). The composite hardness, for $d > h$, can be written

$$H_c = H_s + \frac{3h^2(1 - (1 + \cot^2\phi)h/(3d))}{d^2(2\tan\phi - 1)}(H_f - H_s) \tag{4}$$

where ϕ is the semi-angle of a conical indenter. The coefficient of $H_f - H_s$ leads in second order in h/d, in contrast with the Jönsson–Hogmark model (eqn. (2)). A different expression holds for $d < h$.

The volume mixture model was subsequently developed by Burnett and Rickerby [9, 10] such that the plastic volumes were not confined to the hemisphere under the indenter but were related to the plastic volumes in the spherical cavity model [16], according to which the plastic zone radius is given by the elastic and plastic properties of the material. The revised geometry is shown in Fig. 2(b) for a hard film on a soft substrate. The radius of the plastic zone in the film material is smaller than that for the substrate material. Accordingly, the ratio of film plastic volume to substrate plastic volume is less than that found in the original model, for a hard film on a soft substrate. Similar arguments can be applied to the case of a soft film on a hard substrate. However, it was recognized that the plastic radii in each material are influenced by each other and are not simply given by the spherical cavity model. This was allowed for by the modification of one or other of the terms in eqn (3) by an additional coefficient χ^3, which was fitted to data The model was also extended, empirically, to allow for the indentation size effect [10], whereby the hardness depends on indentation depth even for uncoated substrates [21, 22]. The most recent development of the model has been to

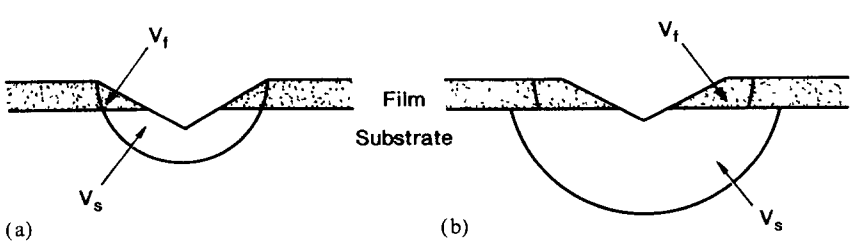

Fig 2 Geometries used in volume mixture law of composite hardness (a) scheme in ref 8, (b) scheme in ref 9

introduce a more realistic geometry whereby the film is allowed to penetrate into the substrate [11]. The approach has been used to interpret a wide range of experimental data [10, 11].

However, whilst the combination of hardnesses according to the areas supporting the load is intuitively appealing, the volume mixture model lacks an equivalent argument to justify the combination of hardness values according to the relative plastic volumes. Superficially, it would appear from eqn. (3) that the total indentation work has been divided into parts due to the deformation of the film and substrate, but this is not a correct interpretation. The total work done would involve the indentation volumes, and not the plastically deformed volumes.

To sum up, available models of the composite hardness of a coated substrate are not based soundly in theory. What seems to be missing in the development of these models is a clear reference to the analytical work which has been applied to the indentation of bare substrates [15–20]. Such work, based on spherical cavity analysis, has improved understanding in that area and might be similarly useful in the study of the coated substrate problem.

3. Spherical cavity analysis

A particularly fruitful approach to the modelling of the indentation of surfaces has been to make use of the known stress–strain fields around a pressurized spherical cavity in an elastic, perfectly plastic material [16]. In spite of the obvious differences in geometry (in particular the free surface and the non-spherical indentation volume in the plane surface case), the predicted dependence of hardness on Young's modulus and yield stress of the substrate material is quite successful [15, 17, 18, 20]. A natural extension of this approach is to consider a pressurized spherical cavity with a shell of film material separating the cavity from the bulk substrate, and to use the geometry as a model for the indentation of a coated substrate. In this section we consider the coated cavity problem, and the connection with plane surface indentation is made in Section 4.

The geometry of the problem is illustrated in Fig. 3(a). A spherical cavity of radius a, containing a fluid at some pressure p, exists within a bulk material with Young's modulus E_s, Poisson's ratio ν_s and yield stress Y_s. Between the cavity and the bulk material is a spherical shell of thickness $t-a$ with material properties E_f, ν_f and Y_f. The shell will be referred to as the film, while the bulk material is denoted the substrate. Both materials are assumed to be elastic, perfectly plastic.

As the cavity expands, a number of deformation regimes may be encountered, depending on the relative material properties. Initially, all strains are elastic, until plastic yield begins at the inner radius of either the film or the substrate. Further expansion of the cavity then increases the size of the plastic zone. It may be possible for both materials to have regions of elastic and plastic deformation, or for the film to be completely plastic while the substrate remains elastic. Eventually, the film yields completely, and the plastic zone penetrates well into the substrate. The stress–strain fields for the various situations can be obtained using the methods of Hill [16], although the existence of the different deformation regimes complicates the analysis, as we now show.

3.1. Elastoplastic substrate

Let us begin by considering the simplest case, where the whole of the film, and the substrate out to a radius c_s, are plastic. The fundamental equation which determines the stress field in the spherical geometry is [16]

$$\frac{d\sigma_r}{dr} = \frac{2(\sigma_\theta - \sigma_r)}{r} \tag{5}$$

where σ_r and σ_θ are the radial and tangential principal components of the stress tensor, both functions of the radius r only. Symmetry requires the remaining principal stress σ_ϕ to be equal to σ_θ. The Tresca condition for plastic yield requires that $\sigma_\theta - \sigma_r = Y$, where Y is the appropriate yield stress. This criterion simplifies the analysis, although the von Mises criterion would perhaps be more realistic. The two criteria, however, usually lead to similar results.

For plastic deformation, eqn. (5) gives the stress field

$$\sigma_r = 2Y \ln r + K \tag{6}$$

whereas for elastic deformation the equivalent general solution is [23]

$$\sigma_r = \frac{A}{r^3} + B \tag{7}$$

and

$$\sigma_\theta = -\frac{A}{2r^3} + B \tag{8}$$

where K, A and B are constants.

Imposing continuity of σ_r at $r = a$, t and c_s gives the following equations:

$$-p = 2Y_f \ln a + K_f \tag{9}$$

$$2Y_f \ln t + K_f = 2Y_s \ln t + K_s \tag{10}$$

$$2Y_s \ln c_s + K_s = \frac{A_s}{c_s^3} + B_s \tag{11}$$

where the subscripts f and s, denoting the film and substrate respectively, have been added to the various constants.

Continuity of σ_θ at $r = c_s$ similarly gives

$$2Y_s \ln c_s + K_s + Y_s = \frac{A_s}{2c_s^3} + B_s \tag{12}$$

so that

$$A_s = -\tfrac{2}{3} Y_s c_s^3 \tag{13}$$

We also impose a boundary condition of zero radial stress as $r \to \infty$, so that $B_s = 0$. Combining the above equations yields an expression for the pressure in terms of the plastic state:

$$p = \tfrac{2}{3} Y_s + 2Y_s \ln\left(\frac{c_s}{a}\right) + 2(Y_f - Y_s) \ln\left(\frac{t}{a}\right) \tag{14}$$

In order to determine c_s, we need to consider an incremental displacement field $\delta u(r)$, and a corresponding change δc_s, in the substrate plastic zone radius. The following equation for the volume strain is valid everywhere:

$$\delta\epsilon_r + \delta\epsilon_\theta + \delta\epsilon_\phi = \frac{\mathrm{d}(\delta u)}{\mathrm{d}r} + \frac{2\,\delta u}{r} = \frac{1-2\nu}{E}(\delta\sigma_r + \delta\sigma_\theta + \delta\sigma_\phi) \tag{15}$$

with appropriate values of parameters. The strain increments have been related to δu in the usual way. In $t < r < c_s$, we find, using eqns (6), (11) and (13) that

$$\frac{\mathrm{d}v}{\mathrm{d}r} + \frac{2v}{r} = \frac{6Y_s(1-2\nu_s)}{E_s}\left(\frac{v}{r} - \frac{1}{c_s}\right) \tag{16}$$

where $v = \delta u / \delta c_s$. For the elastic region in $r > c_s$, we have

$$\delta\epsilon_\theta = \frac{v\,\delta c_s}{r} = \frac{Y_s(1+\nu_s)}{E_s}\left(\frac{c^2}{r^3}\delta c_s - \frac{c^3}{r^4}\delta u\right) \tag{17}$$

so that, to first order in Y_s/E_s,

$$v = \frac{(1+\nu_s)Y_s}{E_s}\frac{c_s^2}{r^2} \qquad r > c_s \tag{18}$$

Now eqn. (16) can be solved, again to first order in Y_s/E_s, with continuity at $r = c_s$, to yield

$$v = \frac{3Y_s(1-\nu_s)}{E_s}\frac{c_s^2}{r^2} - \frac{2Y_s(1-2\nu_s)}{E_s}\frac{r}{c_s}, \tag{19}$$

which is similar to a result obtained by Hill for an uncoated spherical cavity [16].

A similar procedure leads to an equation for v in $a < r < t$, using eqns. (6), (10), (11) and (13):

$$\frac{\mathrm{d}v}{\mathrm{d}r} + \frac{2v}{r} = \frac{6(1-2\nu_f)}{E_f}\left(\frac{Y_f v}{r} - \frac{Y_s}{c_s} + \frac{(Y_s - Y_f)}{t}\frac{\mathrm{d}t}{\mathrm{d}c_s}\right). \tag{20}$$

The solution for v in this region, with suitable continuity at $r = t$, again to first order in Y_s/E_s, is

$$v = \frac{3Y_s(1-\nu_s)}{E_s}\frac{c_s^2}{r^2} - \frac{2Y_s(1-2\nu_f)}{E_f}\frac{r}{c_s} + \frac{2Y_s t^3}{c_s r^2}\left(\frac{1-2\nu_f}{E_f} - \frac{1-2\nu_s}{E_s}\right) \tag{21}$$

So, applying this solution at $r = a$, where $\delta u = \delta a$, and letting the increment δa become small, gives an equation for $\mathrm{d}a/\mathrm{d}c_s$, which can be solved to give the ratio c_s/a required in eqn. (14). The complete solution is complicated, but to first order in Y_s/E_s the result is

$$\left(\frac{c_s}{a}\right)^3 = \left\{\frac{3Y_s(1-\nu_s)}{E_s}\left[1 - \left(\frac{t}{c_s}\right)^3\right] + \left(\frac{a_s}{c_s}\right)^3\right\}^{-1} \tag{22}$$

where a_s is the value of a at which $c_s = t$ and the substrate just becomes plastic. For $c_s \gg t > a_s$, this gives simply

$$\left(\frac{c_s}{a}\right)^3 = \frac{E_s}{3Y_s(1-\nu_s)} \tag{23}$$

which, interestingly, does not depend on the properties of the film. The pressure in the cavity, which is identified as the hardness of the film–substrate composite, is therefore

$$p = \tfrac{2}{3} Y_s\left[1 + \ln\left(\frac{E_s}{3(1-\nu_s)Y_s}\right)\right] + 2(Y_f - Y_s)\ln\left(\frac{t}{a}\right) \tag{24}$$

for the elastoplastic substrate regime. The first term corresponds to the hardness of the substrate [17], and the second is the effect of the film.

The solution holds as long as $c_s > t$. This condition can be translated into a lower limit for the cavity radius a, using eqn. (23), although this introduces some error since that result is valid only for $c_s \gg t$.

3.2. Elastoplastic film

Secondly, let us consider the regime where the substrate is completely elastic, but the film is plastic within a radius c_f ($c_f < t$) and elastic beyond. We use the same methods as above. Stress fields analogous to eqns. (6)–(8) can be constructed for the various regions:

$$\sigma_r = \begin{cases} 2Y_f \ln r + K_f & a < r < c_f \quad (25) \\ \dfrac{A_f}{r^3} + B_f & c_f < r < t \quad (26) \\ \dfrac{A_s}{r^3} & r > t \quad (27) \end{cases}$$

Demanding continuity of σ_r at $r = c_f$ and t, together with that of σ_θ at $r = c_f$, provides three equations linking the five unknown quantities. The cavity pressure is now given by

$$p = \tfrac{2}{3} Y_f + 2Y_f \ln\left(\frac{c_f}{a}\right) - B_f \tag{28}$$

involving the unknowns B_f and c_f. These are found by considering an incremental displacement field δu. Starting from eqn. (15), together with eqns. (25)–(27), it can be shown that

$$\frac{dv'}{dr}+\frac{2v'}{r}=\frac{6Y_f(1-2\nu_f)}{E_f}\left(\frac{v'}{r}-\frac{1}{c_f}+\frac{1}{2Y_f}\frac{dB_f}{dc_f}\right) \tag{29}$$

for $a<r<c_f$, with $v'=\delta u/\delta c_f$. In the elastic regions, however, v' can be found directly:

$$v'=\frac{Y_f(1+\nu_f)}{E_f}\frac{c_f^2}{r^2}+\frac{(1-2\nu_f)}{E_f}\frac{dB_f}{dc_f}r \tag{30}$$

for $c_f<r<t$, and

$$v'=-\frac{(1+\nu_s)}{2E_s}\frac{dA_s}{dc_f}\frac{1}{r^2} \tag{31}$$

for $r>t$, both to first order in Y_s/E_s or Y_f/E_f. Requiring continuity for v' at $r=t$, and using $A_f+B_ft^3=A_s$, we find that

$$\frac{dB_f}{dc_f}=G\frac{c_f^2}{t^3}=\frac{Y_f[(1+\nu_s)/E_s-(1+\nu_f)/E_f]}{(1-2\nu_f)/E_f+(1+\nu_s)/2E_s}\frac{c_f^2}{t^3} \tag{32}$$

again to first order in Y/E. Using this result, v' can be found in $a<r<c_f$ by solving eqn. (29) and demanding continuity at $r=c_f$. The solution for v' at $r=a$ then gives the following equation:

$$\frac{da}{dc_f}=\frac{3Y_f(1-\nu_f)}{E_f}\frac{c_f^2}{a^2}-\frac{2Y_f(1-2\nu_f)}{E_f}\frac{a}{c_f}+\frac{(1-2\nu_f)}{E_f}\frac{c_f^3}{t^3}\left(1+\frac{a}{c_f}-\frac{c_f^2}{a^2}\right)G \tag{33}$$

The ratio c_f/a tends to a constant when $c_f\gg a_f$, where a_f is the value of a at which the film just becomes plastic, and so, dropping small terms in eqn. (33), we have

$$\frac{a}{c_f}=\frac{3Y_f(1-\nu_f)}{E_f}\frac{c_f^2}{a^2}-\frac{1-2\nu_f}{E_f}G\frac{c_f^5}{t^3a^2} \tag{34}$$

which gives, to first order in G,

$$\left(\frac{c_f}{a}\right)^3=\frac{E_f}{3(1-\nu_f)Y_f}\left[1+\frac{(1-2\nu_f)}{3(1-\nu_f)}\frac{G}{Y_f}\left(\frac{a}{t}\right)^3\frac{E_f}{3(1-\nu_f)Y_f}\right] \tag{35}$$

Finally, this result, together with an integrated form of eqn. (32), combines with eqn. (28) to give the cavity pressure p in the elastoplastic film regime:

$$p=\tfrac{2}{3}Y_f\left[1+\ln\left(\frac{E_f}{3(1-\nu_f)Y_f}\right)\right]-G\frac{(1+\nu_f)E_f}{27(1-\nu_f)^2Y_f}\left(\frac{a}{t}\right)^3. \tag{36}$$

Once again, the first term represents the hardness of the film material, and the second corresponds to the effect of the underlying substrate. The above solution holds as long as $c_f<t$. This corresponds to an upper limit for the cavity radius a, using eqn (35), although again this introduces a slight error.

We therefore have two expressions for the cavity pressure, valid for two ranges of cavity radius, an elastoplastic film solution, eqn. (36), for small radii, and an elastoplastic substrate solution, eqn. (24), for large radii. The two approximate ranges of validity which have been identified may or may not overlap. This is partly because approximations have been made, but mostly because there are two further elastoplastic regimes which have not been considered. In the case of a soft film on a hard substrate, there will be a regime where the film is fully plastic, but the substrate remains elastic for a range of cavity radius a. For a hard film on a soft substrate, there might be a range of a where both materials develop plastic zones which are separated by a region of elastically deformed film material. I do not propose to treat these regimes here, partly because of their complexity, and partly because the two solutions given above provide an adequate description of the full behavior, as we shall find in the next section.

4. Application to coated substrates

4.1. *Mapping geometries*

The application of stress–strain solutions for the spherical cavity to the case of plane surface indentation necessarily involves some modification of the geometry. The reason why the cavity solution is useful is that it is often found in indentation tests that the displacements are radial, at a sufficient distance from the centre of the indentation, and that the plastic zone, at least for the case of a bare substrate, is approximately hemispherical [24, 25]. Both these features exist in the solution to the cavity problem. The fundamental differences between the two situations are the presence of the free surface, and the shape of the indenter. However, the success of the spherical cavity models suggests that these differences do not spoil the analogy, at least for hard substrates.

The main uncertainty in applying the cavity model to the indentation of bare substrates is in identifying the inner radius a. Two approaches have been used. Johnson [17] took a to be the radius of the indentation impression at the surface, for a conical or wedge indenter. The hemisphere of material beneath the indenter within this radius was taken to behave like a fluid under a hydrostatic pressure. An alternative approach, suggested by Chiang *et al.* [18], is to identify a with the radius of a hemisphere which has the same volume as the indentation. This implies that the displacements at a large enough distance away from the centre of the indentation do not depend on the indenter shape, but only upon the indented volume. The underlying impli-

cation is that the radius of the plastic zone is controlled by the total plastic work done, which depends on the indented volume but not on the shape. There is some evidence to support this conjecture [18].

The approach of Chiang *et al.* is used here, so that the radius a is related to the depth of indentation d according to

$$a = d(\tfrac{1}{2}\tan^2\phi)^{1/3} \qquad \text{(cone)} \tag{37}$$

or

$$a = d\left(\frac{2}{\pi}\tan^2\phi\right)^{1/3} \qquad \text{(pyramid)} \tag{38}$$

where ϕ is the semi-included angle of a conical indenter, or half the angle between opposite faces of a pyramidal indenter.

The remaining geometrical question concerns the radius t. The approach which seems most sensible is to set

$$t = a + h\sin\phi \tag{39}$$

where h is the thickness of the film. The motivation for this choice is to keep the thickness of the film the same in the two geometries, as illustrated in Fig. 3(b).

The ratio t/a is now written, for a pyramidal indenter, for example, as

$$\frac{t}{a} = 1 + \frac{h}{d}\frac{\sin\phi}{(2/\pi)^{1/3}\tan^{2/3}\phi} \tag{40}$$

which can be inserted into eqn. (24) or eqn. (36) to obtain p, which is identified as the composite hardness as a function of indentation depth d for a given film thickness h. These expressions will be tested in the next section.

4 2. *Comparisons with other models and experiment*

For small h/d, eqn. (40) together with eqn. (24) gives

$$H_c = H_s + (H_f - H_s)\left[\frac{2Dh}{3d} - \frac{D^2h^2}{3d^2} + O\left(\frac{h^3}{d^3}\right)\right] \tag{41}$$

where D is the expression $(\sin\phi)/[(2/\pi)^{1/3}\tan^{2/3}\phi]$ in eqn. (40), and the approximation $H \approx 3Y$ has been used. This expression corresponds in form to the Jönsson–Hogmark model, eqn. (2). The coefficients of the h/d and $(h/d)^2$ terms in the square brackets in eqn. (41) are, however, 0.393 and 0.115 for $\phi = 68°$, compared with 0.146 and 0.005 respectively for $H_f \gg H_s$ in eqn. (2). The version of the volume mixture law given in eqn. (4) lacks a term in h/d, but the equivalent coefficient of the $(h/d)^2$ term is 0.759. Numerically, the predictions of the area and volume mixture models show similar behaviour, with the greatest differences at small indentation depths [10]. We now compare the Jönsson–Hogmark model and the coated cavity model in a particular case.

Laursen and Simo [4] used a finite element numerical approach to study the indentation of coated surfaces indented by conical indenters with an apex angle of 136°. They studied films of aluminium on silicon and silicon on aluminium and the material properties used are given in Table 1. The points in Fig 4 are representative of their depth-dependent hardness calculations for a 1 μm coating of silicon on aluminium. The Jönsson–Hogmark

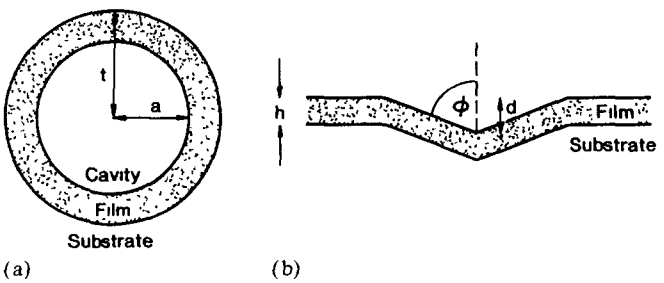

Fig. 3 (a) Geometry of coated spherical cavity, and (b) relation to coated plane surface geometry

TABLE 1 Material properties used in the various calculations

Material	E (GPa)	Y (MPa)	ν	Reference
Aluminium	75 9	485	0 33	[4]
Silicon	127	4410	0 278	[4]
Nickel–boron alloy	100	1280	0 36	[26, 27]
SAE 1018 steel	200	200	0 3	[27]
Chromium	279	400	0.21	[6, 27]
AISI 52100 steel	200	217	0 30	[6]
High strength, low alloy (HSLA) steel	200	170	0 30	[6]
Stainless steel	200	630	0 30	[6]
Copper	130	310	0 343	[6, 27]

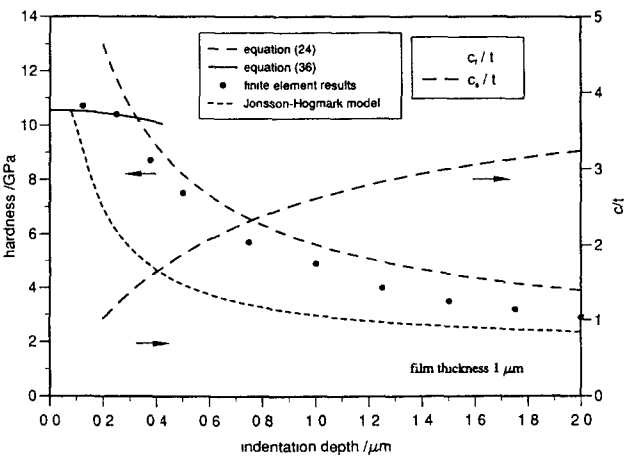

Fig 4 Hardness of aluminium coated with silicon for a range of indenter depths, comparing the finite element calculations [4] with the coated cavity model and the area mixture law [6] Plastic zone sizes against penetration are also shown

model predictions for $H_f \gg H_s$ are shown as a broken curve (short dashes). The broken curve (long dashes) and full curves are the predictions of the coated cavity model for the elastoplastic substrate (eqn. (24)) and elastoplastic film (eqn. (36)) regimes respectively The model gives better agreement than the Jönsson–Hogmark model, especially for the depth corresponding to the transition between regimes. At larger depths, however, the hardness is overestimated.

Each coated cavity model solution is shown for a range of depths corresponding to the conditions $c_s \geqslant t$ and $c_f \leqslant t$ which are attached to each case. The evolution of the plastic radii, normalized by t, according to eqns. (23) and (35), is also shown in Fig. 4. The ranges overlap in this example. In reality, a more complicated elastoplastic behaviour occurs near the cross-over, and eqns. (24) and (36) are not valid there, but the two curves shown provide an adequate description of the hardness dependence, and a more detailed consideration of the intermediate situation is not justified.

The numerical indentation of a 1 μm aluminium film on a silicon substrate compares less well with the coated cavity model. The appropriate hardness solutions given by eqns. (24) and (36) are shown in Fig. 5 for this case and are compared with the finite element results. The ranges for the two solutions do not overlap in this case. The model predicts too high a hardness for most of the range of depths. The reason for this is that the soft aluminium does not deform under indentation in the manner assumed in the model, instead it flows outwards and upwards around the indenter to produce a pile-up. The transition from radial flow to this sort of flow, better modelled by the slip-line field solution [28], is well established [17] For such a deformation pattern, the hardness is approximately equal to three times the yield stress. Yield of the harder substrate does not occur until the indenter has penetrated the film, the film material deforming to produce a bulge at the surface. The composite hardness is best modelled in this situation by an area mixture law, but based on indenter penetration of the film rather than the geometry used by Jönsson and Hogmark (*i.e.* more like Fig. 2 than Fig. 1). For conical or pyramidal indenters, such a model predicts that

$$H_c = H_s + (H_f - H_s)\left(\frac{2h}{d} - \frac{h^2}{d^2}\right) \qquad (42)$$

for $d > h$ and $H_c = H_f$ otherwise. The dotted curve in Fig. 5 shows the predictions of this model, with H_f given by $3Y_f$ [28], and H_s given by the first term in eqn. (24). It provides a much better fit to the finite element results than the coated cavity model does, although again the tendency is to overpredict the hardness as the indentation depth increases.

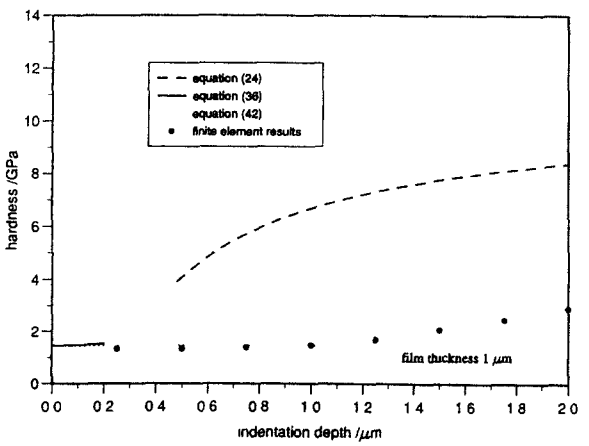

Fig. 5 Hardness of silicon coated with aluminium for a range of indenter depths, comparing finite element calculations [4] with the coated cavity model, eqns. (24) and (36), and the modified area mixture law, eqn. (42)

It should be noted that the aluminium was allowed to harden in the simulations of Laursen and Simo. This cannot be catered for in the cavity model since the materials are taken to be elastic, perfectly plastic; allowance for hardening would, however, worsen the fit to eqn. (42).

Lebouvier *et al.* [26] have developed a two-dimensional rigid-block model to describe the indentation of a coated substrate and have carried out a programme of indentation measurements to test their conclusions. The data can also be used to test the coated cavity model. We concentrate on the measurements made for a coating of a hard nickel–boron alloy on softer SAE 1018 steel. However, ref. 26 did not provide complete material properties, only the ratio of yield stresses, which is all that is needed in the rigid-block model. Estimates of the remaining parameters are given in Table 1. A comparison of measured and predicted hardnesses, for various ratios of coating thickness h to pyramidal indenter impression semiwidth $w = d \tan \phi$, is shown in Fig. 6. The predictions shown are not very sensitive to the choices of material properties. The model provides a reasonable description of behaviour for this case, although for deep penetrations the hardness is again overestimated. The Jönsson–Hogmark model provides a better fit for large indentation depths but underpredicts in the intermediate range.

A larger set of measurements of the hardness of coated substrates was used by Jönsson and Hogmark [6] to test their model. Various substrates were given 1 μm chromium coatings and tested with a pyramidal indenter. In each case the film was harder than the substrate. The material properties are given in Table 1 and the predicted and measured hardnesses, for various penetrations, are shown in Fig. 7. The model is reasonably successful in accounting for the behaviour, although

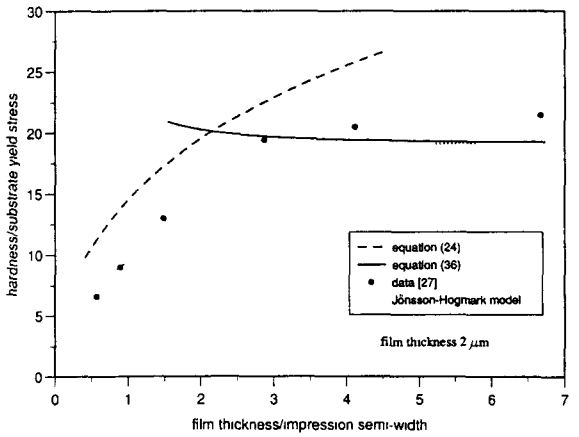

Fig 6 Comparison of coated cavity model predictions and data for a steel coated with a strong nickel–boron alloy The Jonsson–Hogmark model provides a better fit at the large indentation extreme, but underpredicts elsewhere

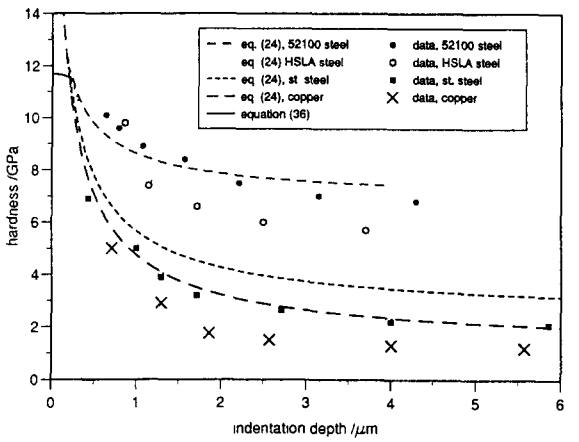

Fig 7 Comparison of model predictions and hardness data for various materials coated with a 1 μm film of chromium.

there is once again a tendency to overpredict the hardness for deep indentations. The results may be compared with Fig. 9 in ref. 6.

An even wider data set has been reported in ref. 10, describing titanium nitride and tungsten–titanium carbide coatings on a variety of substrates. However, Burnett and Rickerby [10] found that the volume mixture model, which they used to interpret the results, required empirical modification to include a strong indentation size effect (ISE) arising from the coating materials. The study of these results using the coated cavity model would therefore not be useful at this stage, since an allowance for the ISE is not yet included. The materials involved in the other tests discussed in this section are metallic, which are generally less affected by the ISE. Consideration of the data in ref. 10 must await the inclusion of the ISE within the coated cavity model.

5. Discussion

This paper has sought to establish a rigorous basis for predicting the hardness of a coated substrate, as a function of the coating thickness and the indentation depth. The approach used is indirect, in that first a related problem with a different geometry is solved, namely the expansion of a spherical cavity within a bulk material, with a coating of a different material at the interface. Both materials are taken to be elastic, perfectly plastic. This analysis uses the methods of Hill [16], who treated the uncoated spherical cavity problem. His stress–strain solution was subsequently used, with some success, to describe the indentation of uncoated surfaces [15, 17–20]. The natural development which has been followed in this paper is to use the solution to the coated cavity problem to model the hardness of coated plane surfaces.

The material displacements in spherical cavity problems are radial, by symmetry. The reason for the success of Hill's solution seems to be that the displacements produced by the indentation of plane surfaces, at a sufficient distance from the indenter surface, are approximately radial in many cases. This provides the crucial similarity between the cavity case and the plane surface case.

The indentation displacement pattern is rather different when the ratio of Young's modulus to yield stress exceeds a certain threshold. The flow of material away from the indenter is then no longer radial but is directed more towards the free surface, producing a pile-up. This is the point at which cavity models cease to be useful in describing surface indentation, and a slip-field model of indentation becomes more appropriate [28]. The hardness is then approximately equal to three times the yield stress. Spherical cavity models are therefore not suitable for describing the indentation of soft materials (low yield stress) and this restriction holds both for soft substrates and for surfaces coated with soft films.

Nevertheless, in most practical cases, the film material is hard, often a ceramic, and a cavity model is then a suitable description. Furthermore, a soft substrate, which would normally pile up, might deform radially under the constraint of a hard surface film, which would make a cavity model appropriate even for these materials. In the calculations described in the last section, the predictions of the coated cavity model were used irrespective of the E/Y ratio of the material However, if E_s is subject to an upper limit equal to $3Y_s$, then some of the predicted hardnesses in Figs 4–7 would be reduced slightly.

The stress–strain solutions found here for the case of an expanding coated spherical cavity have been applied to the indentation of plane coated substrates by making two geometrical correspondences, both of which are subject to some uncertainty Adjusting these assumptions is possible and might improve the fit to experiment, but at present the following procedure is followed. Firstly, the indentation volume, which depends on the shape of the indenter, is set equal to the volume of a hemisphere, which identifies the cavity radius in the analytic solution. Secondly, the thickness of the film when pressed into the substrate is identified with the thickness of the coating in the cavity problem. The relationship between the cavity pressure and the cavity size is then translated into a indentation depth dependence for the coated substrate hardness. Several such relationships hold valid for various ranges of depth, corresponding to various elastoplastic regimes in the cavity problem. Equations (24) and (36) are two such expressions, describing situations where a single plastic zone is contained within an elastic zone, with the edge of the plastic zone lying in the substrate and film respectively. These two provide a reasonable coverage of the entire range of indentation depths.

The theory has been compared with other simple models. Analytically, the solutions differ in detail compared with the area [6] and volume [7–11] mixture models, but similarly shaped curves of hardness against depth are obtained. For shallow indentations, the apparent hardness is close to that of the film, but beyond a critical penetration, equal to about one fifth of the film thickness, the hardness changes rapidly towards that of the substrate. In contrast with both the area and the volume mixture models, however, the solutions are based upon a rigorous theoretical development, albeit for a spherical geometry

No attempt has yet been made to include the indentation size effect within the model. This depth dependence of hardness, even for uncoated substrates, has yet to be explained satisfactorily and has only been included empirically within the area and volume models. A similar procedure may be necessary for the coated sphere model.

The predictions of the model have been compared with data from several indentation studies, both numerical and experimental. In general, the model can account for the hardness trends for hard films on soft substrates but not vice versa. This is because the assumption of radial displacements, implicit within cavity models, fails for softer materials which can bulge at the free surface in a coated plane surface geometry.

The model assumes elastic perfectly plastic deformation behaviour for the materials involved, which can be unrealistic. A development to include power law hardening may be possible, perhaps using an approach similar to that of Matthews [29].

6. Conclusions

The problem of the expansion of a pressurized sphere, coated with a film material, within a bulk substrate material, has been solved, assuming elastic, perfectly plastic material properties. This situation has been used to represent the indentation of a coated plane surface, and the analogy has yielded a model of the depth dependence of the hardness of the coated surface. The theory predicts a critical indenter penetration up to which the hardness is reasonably unaffected by the substrate properties, but beyond which the hardness changes rapidly. The model provides a better description of hard films on soft substrates than vice versa The present model is more soundly based in theory than some other models but shows many of the same features and provides a good description of finite element calculations and experimentally measured hardnesses. At present, it lacks an allowance for the indentation size effect, although it may be possible to include this empirically. Using this model, it should be possible to interpret the loading curves arising from the indentation of coated substrates, and to determine the film parameters required to provide the desired hardness in a particular application

Acknowledgment

This work was funded by the Corporate Research programme of AEA Technology.

References

1 I. M. Hutchings, *Tribology: Friction and Wear of Engineering Materials*, Edward Arnold, London 1992, Chapter 8
2 S Chatterjee, T. S. Sudarshan and S. Chandrasekhar, *J Mater. Sci*, *27* (1992) 1989
3 T F Page and J C. Knight, *Surf. Coat. Technol*, *39–40* (1989) 339.
4 T A. Laursen and J C. Simo, *J Mater. Res.*, *7* (1992) 618.
5 H. Bückle, in J. W. Westbrook and H. Conrad (eds.), *The Science of Hardness Testing and its Research Applications*, American Society for Metals, Metals Park, OH, 1973, p. 453.
6 B Jönsson and S. Hogmark, *Thin Solid Films*, *114* (1984) 257
7 P. M. Sargent, *Ph.D. Thesis*, University of Cambridge, 1979
8 P. J. Burnett and T. F. Page, *J Mater. Sci.*, *19* (1984) 845.
9 P. J Burnett and D. S. Rickerby, *Thin Solid Films*, *148* (1987) 41.
10 P. J Burnett and D. S. Rickerby, *Thin Solid Films*, *148* (1987) 51
11 S. J Bull and D. S Rickerby, *Surf. Coat. Technol.*, *42* (1990) 149
12 J. Halling, *Thin Solid Films*, *108* (1983) 105.
13 J A Ogilvy, *Rep. AEA-InTec-1218*, January 1993 (AEA Industrial Technology, Harwell Laboratory).
14 M. J Matthewson, *J. Mech. Phys. Solids*, *29* (1981) 89.
15 D. M. Marsh, *Proc. R. Soc. London, Ser A*, *279* (1964) 420.
16 R Hill, *The Mathematical Theory of Plasticity*, Clarendon, Oxford 1950, Chapter 5
17 K. L Johnson, *J Mech. Phys. Solids*, *18* (1970) 115

18 S S. Chiang, D. B Marshall and A G Evans, *J Appl Phys*, *53* (1982) 298
19 B R Lawn, A. G Evans and D B Marshall, *J Am. Ceram. Soc*, *63* (1980) 574.
20 K Tanaka, *J Mater. Sci*, *22* (1987) 1501
21 D Tabor, in P. J Blau and B R Lawn (eds), *Microindentation Techniques in Materials Science and Engineering*, ASTM Spec Tech Publ 889, 1985 (American Society for Testing and Materials, Philadelphia, PA)
22 S J Bull, T F. Page and E. H Yoffe, *Philos Mag Lett*, *59* (1989) 281
23 S Timoshenko, *Theory of Elasticity*, McGraw-Hill, New York, 1934, p 325.
24 L E Samuels and T O Mulhearn, *J Mech Phys. Solids*, *5* (1957) 125
25 T O. Mulhearn, *J Mech Phys. Solids*, *7* (1959) 85
26 D Lebouvier, P. Gilormini and E Felder, *J Phys D.*, *18* (1985) 199
27 E A Brandes (ed.), *Smithell's Metals Reference Book*, 6th edn. Butterworth, London, 1982, Chapter 15
28 D Tabor, *The Hardness of Metals*, Clarendon, Oxford 1951
29 J R Matthews, *Acta Metall*, *28* (1980) 311